Monitoring seismic wave velocity changes associated with the Mw 7.9 Wenchuan earthquake: increasing the temporal resolution using curvelet filters

L. Stehly, B. Froment, M. Campillo, Q. Y. Liu, J. H. Chen

▶ **To cite this version:**

L. Stehly, B. Froment, M. Campillo, Q. Y. Liu, J. H. Chen. Monitoring seismic wave velocity changes associated with the Mw 7.9 Wenchuan earthquake: increasing the temporal resolution using curvelet filters. Geophysical Journal International, 2015, 201 (3), pp.1939 - 1949. ⟨10.1093/gji/ggv110⟩. ⟨hal-01381373⟩

HAL Id: hal-01381373

https://hal.science/hal-01381373v1

Submitted on 17 Jun 2021

HAL is a multi-disciplinary open access archive for the deposit and dissemination of scientific research documents, whether they are published or not. The documents may come from teaching and research institutions in France or abroad, or from public or private research centers.

L'archive ouverte pluridisciplinaire **HAL**, est destinée au dépôt et à la diffusion de documents scientifiques de niveau recherche, publiés ou non, émanant des établissements d'enseignement et de recherche français ou étrangers, des laboratoires publics ou privés.

HAL Authorization

Geophysical Journal International

Geophys. J. Int. (2015) **201,** 1939–1949
GJI Seismology

doi: 10.1093/gji/ggv110

Monitoring seismic wave velocity changes associated with the Mw 7.9 Wenchuan earthquake: increasing the temporal resolution using curvelet filters

Laurent Stehly,[1,2] Bérénice Froment,[3] Michel Campillo,[2] Qi Yuan Liu[4] and Jiu Hui Chen[4]

[1] *Géoazur, Université de Nice Sophia-Antipolis, CNRS, Observatoire de la Côte d'Azur,* 250 *rue Albert Einstein, Sophia Antipolis F*-06560 *Valbonne, France. E-mail: stehlyl@ujf-grenoble.fr*
[2] *ISTerre, Université Joseph Fourier de Grenoble, CNRS, BP* 53, *F*-38041 *Grenoble cedex 9, France*
[3] *Earth, Atmospheric and Planetary Sciences Department, Massachusetts Institute of Technology, Cambridge, MA, USA*
[4] *State Key Laboratory of Earthquake Dynamics, Institute of Geology, China Earthquake Administration, Beijing, China*

Accepted 2015 March 3. Received 2015 March 2; in original form 2014 July 21

SUMMARY

The aim of this study is to improve the temporal resolution of seismic wave velocity variations measured using ambient noise correlations. We first reproduce the result obtained by Chen *et al.* using a network of 21 broad-band stations ideally located around the fault system activated during the Wenchuan earthquake.We measure a velocity drop of 0.07 per cent that was associated with the main shock, with a temporal resolution of 30 days. To determine whether this velocity drop is co-seismic or post-seismic, we attempt to increase the temporal resolution of our observations. By taking advantage of the properties of the curvelet transform, we increase the signal-to-noise ratio of the daily correlations computed between each station pair. It is then possible to measure the velocity drop associated with the Wenchuan earthquake with a temporal resolution of 1 day. This shows that the velocity drop started on 2008 May 12, which was the day of the earthquake, and the velocity reached its lowest value 2 days after the main shock. Moreover, there was a second velocity drop on 2008 May 27, which might relate to strong aftershocks.

Key words: Seismicity and tectonics; Seismic tomography.

1 INTRODUCTION

In recent years, the use of seismic ambient noise correlations has opened up a new way to monitor seismic wave velocity changes associated with earthquakes (Wegler & Sens-Schonfelder 2007; Brenguier *et al.* 2008; Chen *et al.* 2010; Zaccarelli *et al.* 2011; Froment *et al.* 2013). The method used in these studies has consisted of repeatedly extracting the Green's function of the medium between (ideally) pairs of receivers of a dense network by correlating the ambient noise records. Seismic wave speed changes within the medium can be monitored by analysing the coda part of the reconstructed Green's function (Stehly *et al.* 2008) using either the doublet method (Poupinet *et al.* 1984), the stretching method (Lobkis & Weaver 2003; Sens-Schönfelder & Wegler 2006) or the instantaneous phase method (Corciulo *et al.* 2012).

The Mw 7.9 Wenchuan earthquake that occurred in May 2008 is of particular interest as it is one of the largest continental thrust events in the world, and it occurred within a dense network of broad-band stations. Xu *et al.* (2009) showed that the rupture associated with the earthquake propagated over 320 km, from southern Longmen Shan towards the northeast, the hypocenter being localized at 15 km in depth. Chen *et al.* (2010) showed that the main shock was associated with a seismic velocity drop of about 0.08 per cent, which is of the same order as the seismic velocity drop that Brenguier *et al.* (2008) and Zaccarelli *et al.* (2011) reported for the M6.0 Parkfield and the M6.1 L'Aquila earthquakes, respectively.

However, the temporal resolution of these studies was intrinsically limited, as cross-correlations need to be averaged over a sufficiently long time window to provide the Green's function of the medium with reasonable signal-to-noise ratio (Sabra *et al.* 2005; Larose *et al.* 2008). For instance, Chen *et al.* (2010) measured the velocity change associated with the Wenchuan earthquake with a temporal resolution of 30 days. It is therefore not possible to determine with sufficient temporal resolution if the observed changes are co-seismic or post-seismic, or if they occurred before the main shock and could thus be seen as precursors. Similarly, if the velocity change is not instantaneous, its evolution cannot be described over a short timescale.

The aim of this study is thus to increase the temporal resolution of the seismic velocity change measurement to follow daily variations.

© The Authors 2015. Published by Oxford University Press on behalf of The Royal Astronomical Society.

Downloaded from https://academic.oup.com/gji/article/201/3/1939/776465 by guest on 17 June 2021

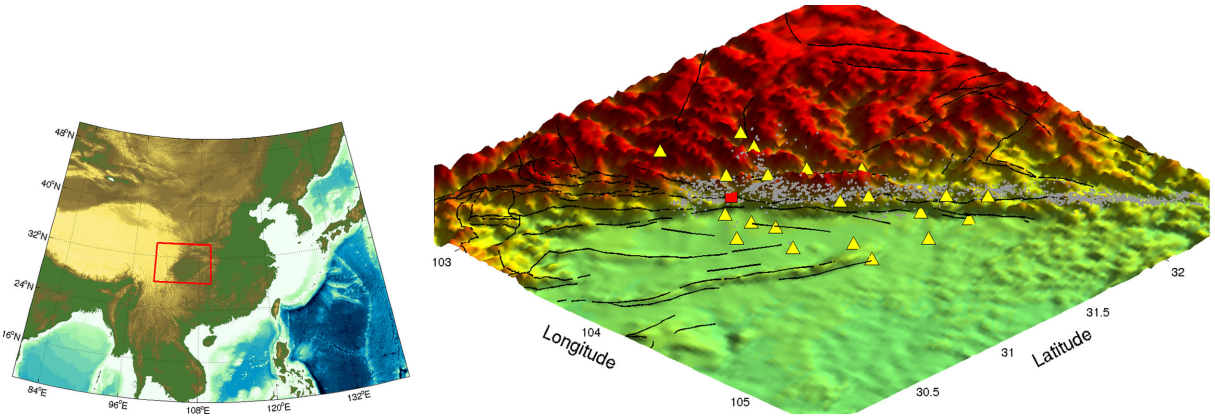

Figure 1. Map showing the 21 broad-band recorders used in this study (yellow triangles). The epicentre of the Mw 7.9 Wenchuan earthquake is indicated by the red square. The rupture associated with the earthquake propagated over 320 km from southern Longmen Shan towards the northeast, the hypocentre being at 15 km in depth. The main faults of the region are indicated by a black line. The aftershocks localized by Chen *et al.* (2009) are shown as grey dots.

We focus specifically on the 1–3 s period band to study the temporal evolution of the upper crust.

We first present the data set and the method used to measure the seismic velocity changes from the noise correlations (Sections 2 and 3). Using a subset of the data used by Chen *et al.* (2010), we reproduce their results using the same method (Section 4). Following the approach of Stehly *et al.* (2011), we then use the curvelet transform to increase the signal-to-noise ratio of the correlations. This allows us to increase the temporal resolution of our observation to 1 day.

2 DATA AND CROSS-CORRELATIONS

We use here a subset of the data used by Chen *et al.* (2010) that consists of 20 months of vertical noise recorded at 21 broad-band stations between 2007 January and 2008 August. These data are part of the Western Sichuan Seismic Array (WSSA) that was run by the Institute of Geology of the China Earthquake Administration, and which was operational for two years (2007 January to 2008 December). The stations used here are ideally distributed around the Longmen Shan fault system, which was activated during the Wenchuan earthquake (Fig. 1). The average interstation spacing was about 30 km and the proximity of these 21 stations to the Wenchuan earthquake make this data set well suited to study the temporal variations of the medium associated with this large earthquake with high temporal resolution.

We processed the noise records in the following way: first, the data were corrected from the instrumental response and decimated to 5 Hz. To downweigh the contribution of energetic signals, such as glitches, earthquakes or ocean storms, we normalized the amplitude of the records in the time domain, by dividing them by their envelope in the 1–3 s period band.

For each station pair, we cross-correlated the normalized vertical records day by day. In the following, we consider that these correlations are an approximation of the Green's function between the stations. We either processed these daily correlations directly or considered them as 5-, 10- or 30-day-stacked correlations to increase the signal-to-noise ratio. The n-day-stacked correlations were computed by stacking the daily correlations with a sliding window of n days. An example of the daily correlations between two stations 60 km apart (KCD01 and KCW05) is shown in Fig. 2.

3 MEASURING VELOCITY CHANGES BY STRETCHING

Our aim is to measure the seismic wave speed change that was associated with the Wenchuan earthquake using ambient noise correlations. We choose to use the stretching method (Lobkis & Weaver 2003; Sens-Schönfelder & Wegler 2006) rather than the doublet method (Poupinet *et al.* 1984; Brenguier *et al.* 2008), as it has been shown to be less sensitive to noise in the data (Hadziioannou *et al.* 2009). This is particularly important, as our aim is to get the highest temporal resolution possible.

In this section, we explain briefly the principle of the stretching method. For detailed explanations, see Hadziioannou (2011).

3.1 Measuring velocity changes by stretching

For each station pair, we define a 'reference' that is simply the sum of all of the daily correlations; that is, the correlation averaged over 20 months. The medium change is then tracked by comparing each correlation of, for instance, 30 days (which we call 'the current correlation' in the following), with the reference.

We specifically use the coda waves that travel through the medium for a longer time than direct waves and are therefore more sensitive to any velocity changes in the medium. In the case of a homogeneous velocity change, the time delay experienced by the wavefield increases linearly with the propagation time.

This means that the coda part of the Green's function measured between two points after the change is either stretched or compressed by a factor $(1 \pm \frac{\delta v}{v})$, with respect to the Green's function measured before the change (see Fig. 3). The relative velocity change $\delta v/v$ at a given date is thus determined as the stretching factor ϵ_0 by which the time axis of the trace at this given date has to be stretched or compressed to obtain the best correlation with the reference trace.

Ideally, the time window used to measure ϵ should start after the direct arrivals and span up to the point where the coda disappears into the noise level. In the 1–3 s period band, we use the coda waves in a window starting at a traveltime corresponding to a velocity of 1.8 km s^{-1} + 20 s and finishing at 120 s (see Fig. 2).

Downloaded from https://academic.oup.com/gji/article/201/3/1939/776465 by guest on 17 June 2021

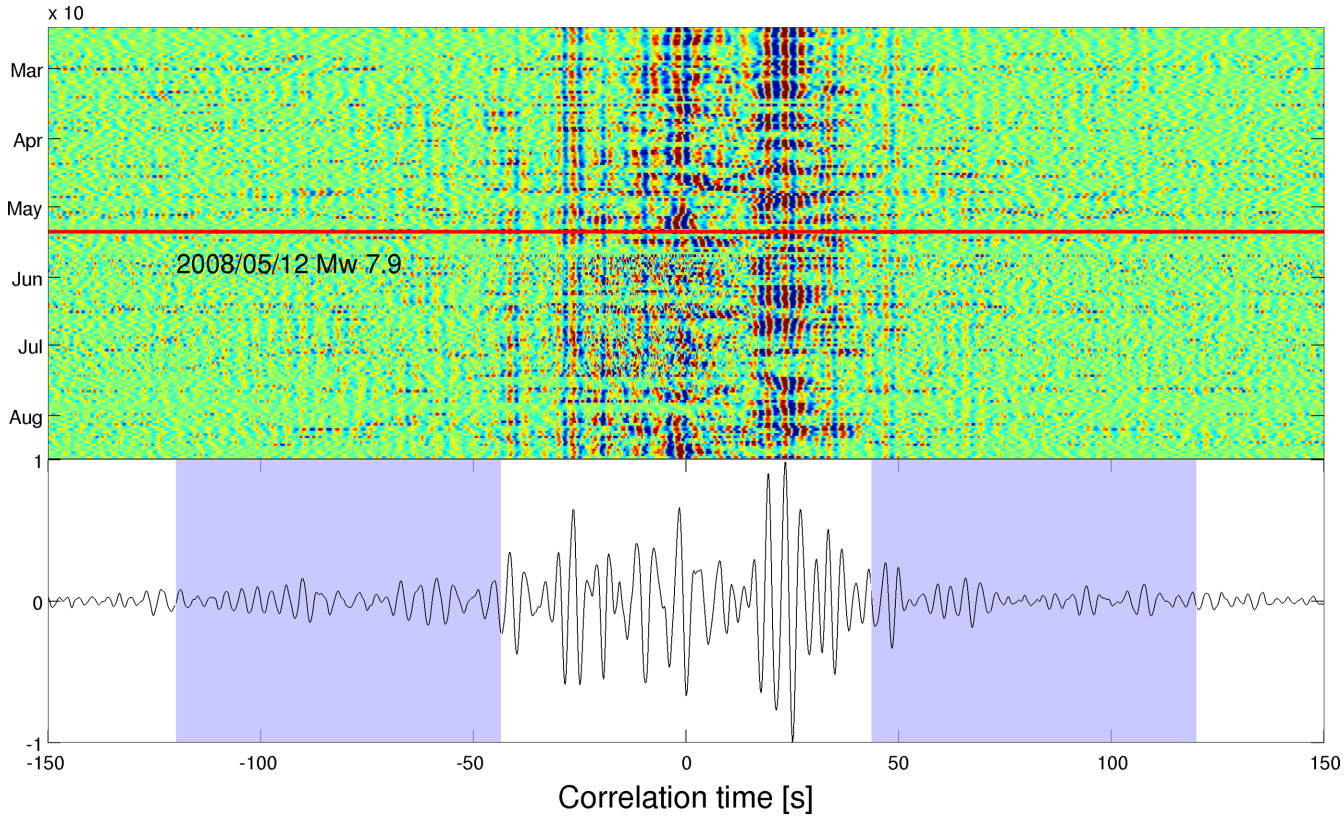

Figure 2. Upper panel: matrix of daily correlations computed between stations KCD01 and KWC05, separated by 60 km. The correlations are filtered in the 1–3 s period band. The red line indicates the date of the Wenchuan earthquake. Lower panel: reference correlation as the sum of all of the daily correlations. The blue shaded area corresponds to coda waves with a velocity $<1.8\,\mathrm{km\,s^{-1}}$ and an arrival time <120 s that are used to measure $\delta v/v$ in the 1–3 s period band.

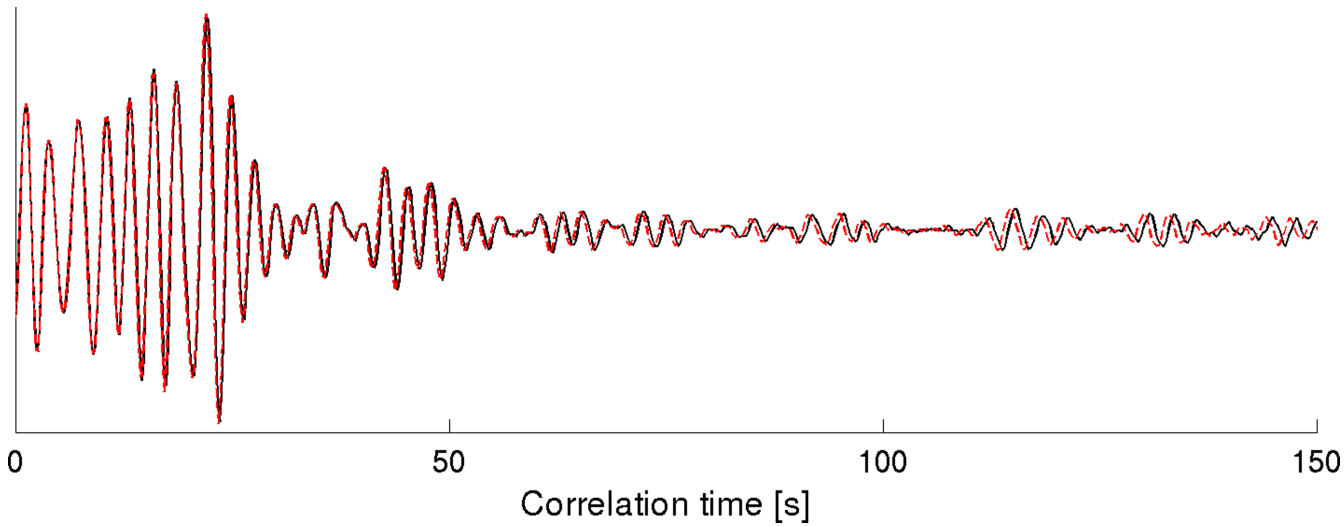

Figure 3. Correlation before (black) and after (red) a homogeneous change in the medium of the seismic velocity $\delta v/v = 0.5$ per cent. The effect of such a change is to stretch the waveform.

3.2 Precision of the velocity change measurements

This way to measure $\delta v/v$ is based on the assumptions that the velocity change is both small and homogeneous, so that the coda waves of the Green's function measured before and after the change differ only by a dilation. Moreover, we assume that the coda waves are equally well reconstructed on the reference and on the current correlation (the n-day stacked correlations). This is true only if the noise sources are stationary and well distributed, and the correlations are stacked over a sufficiently long period of time.

If these assumptions are fulfilled, the waveform of the reference correlation and the stretched current correlation should match perfectly, and the correlation coefficient $C(\epsilon_0)$ should be 1.0. A value <1.0 implies either a change in the noise source, a nonhomogeneous velocity change or a structural change in the medium.

The error of the measure implied by a lack of coherence between the reference and the current correlation was analysed by

Downloaded from https://academic.oup.com/gji/article/201/3/1939/776465 by guest on 17 June 2021

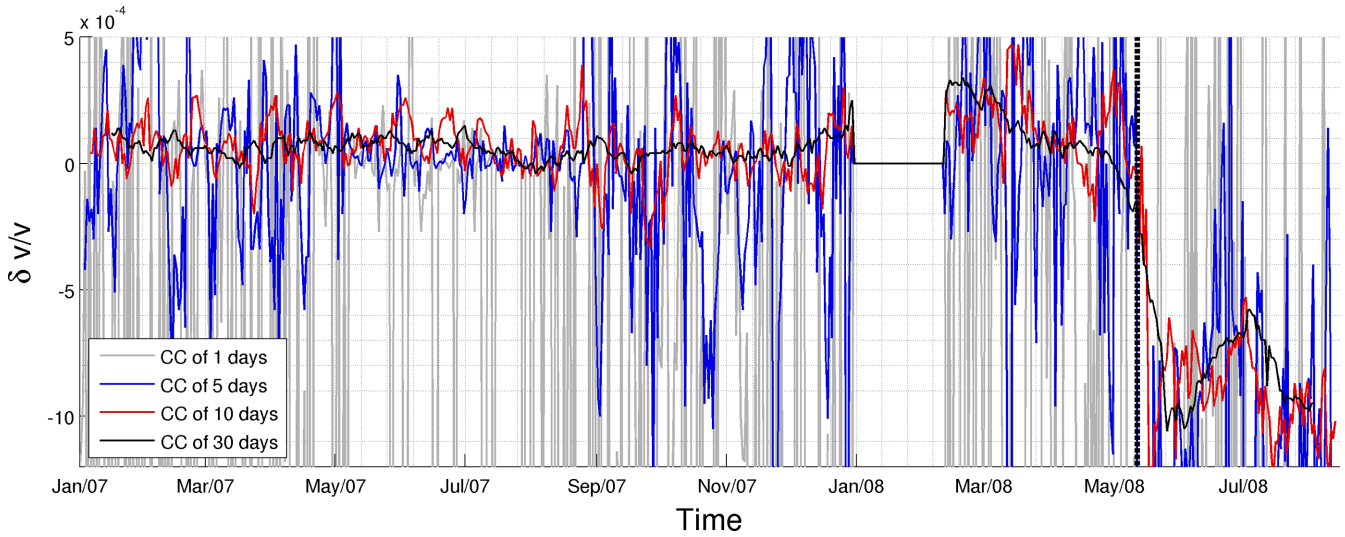

Figure 4. $\delta v/v$ measured by stretching. Results using cross-correlations of 30, 10, 5 or 1 days of noise are shown in black, red, blue and grey, respectively. The vertical dashed line indicates the day of the Wenchuan earthquake.

Table 1. Error on the measurements of the temporal evolution of the seismic velocity. Columns 2 and 3 indicate how the error on the $\mathrm{d}v/v$ measurements and the coherency between the reference correlation and the signal depend on the amount of noise correlated. Note that the velocity drop associated with the Wenchuan earthquake was about $\epsilon_0 = \delta v/v = 0.710^{-3}$.

Amount of noise correlated (days)	rms($\epsilon_{\mathrm{error}}$) 10^{-3}	Average coherency
30	0.14	0.78
10	0.25	0.61
5	0.36	0.49
1	0.94	0.26

Weaver *et al.* (2011). Assuming Gaussian noise sources, the root mean square of the errors of the estimate of the relative dilation $\epsilon_0 = \delta v/v$ between the reference and the current correlation is

$$\mathrm{rms}\ \epsilon_{\mathrm{error}} = \frac{\sqrt{1 - C^2(\epsilon_0)}}{2C(\epsilon_0)} \sqrt{\frac{6T\sqrt{\frac{\pi}{2}}}{\omega_c^2(t_2^3 - t_1^3)}}, \quad (1)$$

where $C(\epsilon_0)$ is the correlation coefficient between the reference and the stretched signal, ω_c is the central frequency in rad s^{-1}, T is the inverse of the frequency bandwidth, and t_1 and t_2 are the beginning and the end of the coda window used, in seconds. This relationship provides an easy way to evaluate the quality of our observations.

4 TEMPORAL VELOCITY CHANGES MEASURED ON RAW CORRELATIONS

The goal of this section is to push the velocity change measurements to their limits and to see what is the best temporal resolution that can be obtained. In particular, we want to know if it is possible to distinguish co-seismic from post-seismic velocity changes.

4.1 Results

The temporal evolution of the coda wave speed in the 1–3 s period band is presented in Fig. 4.

A velocity drop associated with the Wenchuan earthquake of about 0.07 per cent is clearly visible for the measurements performed on correlations of 30 days (Fig. 4, black line). This is in good agreement with the studies of Chen *et al.* (2010) and Zhikun *et al.* (2014).

We attempt to increase the temporal resolution of our observations by using correlations of smaller time windows. As shown in Fig. 4 (red), using correlations of 10-day windows, a velocity drop of about 0.1 per cent is still visible. However with correlations of 5-day or 1-day windows, it is not possible to unambiguously measure any velocity change (Fig. 4, blue and grey, respectively). The results obtained with the daily correlations oscillate rapidly with such a large amplitude that no trend can be detected.

4.2 Assessing the precision of the $\delta v/v$ measurements

As we have seen in the previous section, there is an obvious trade-off between the temporal resolution and the precision of the velocity change measurements. Indeed, the signal-to-noise ratio of the coda waves used to measure $\delta v/v$ scales as the square root of the duration of the noise correlated (Sabra *et al.* 2005; Larose *et al.* 2008). Getting a higher temporal resolution requires the use of correlations computed from shorter durations of data. Coda waves are then reconstructed with lower signal-to-noise ratio, and the coherency between the reference correlation and the signal (the correlation at a given date) is lower. According to eq. (1), this implies that the error on the $\delta v/v$ measurements increases.

The results of the errors and coherencies for the different sliding windows are presented in Table 1. The rms of the error in the estimation of $\delta v/v$ using correlations of 30, 10, 5 and 1 day, are

Downloaded from https://academic.oup.com/gji/article/201/3/1939/776465 by guest on 17 June 2021

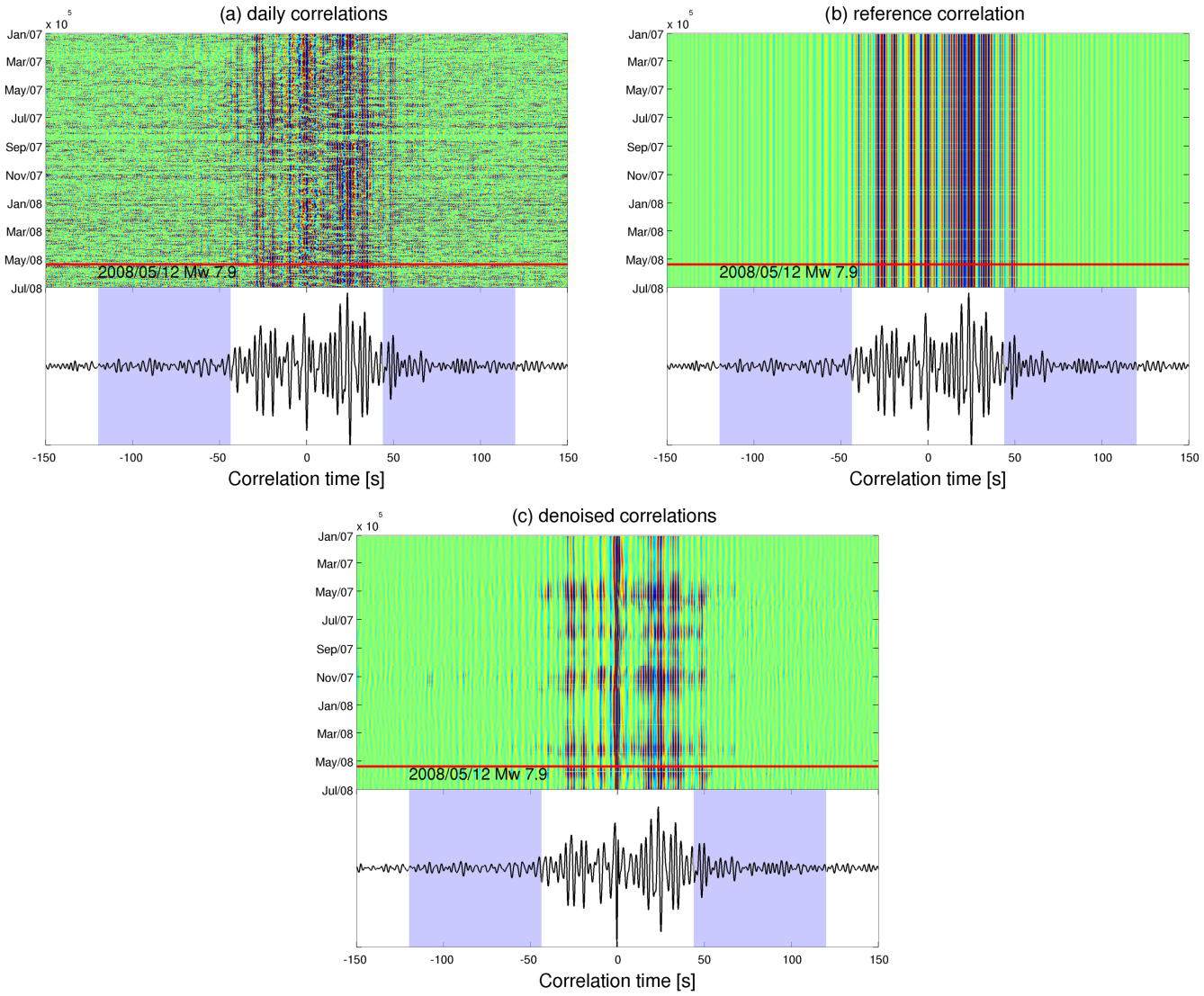

Figure 5. (a) Top panel: matrix $\boldsymbol{C}$ of the daily correlations computed between stations KCD01 and KWC05, filtered in the 1–3 s period band. Lower panel: reference correlation, as the sum of all of the daily correlations. (b) Matrix $\boldsymbol{R}$ where each line is the reference correlation for the station pair KCD01–KWC05. (c) Matrix of the daily correlations denoised using the curvelet filters.

respectively 0.14×10^{-3}, 0.25×10^{-3}, 0.36×10^{-3} and 0.94×10^{-3}. These values of rms (ϵ_{error}) have to be compared to the velocity drop associated with the Wenchuan earthquake, which was about $\epsilon_0 = \delta v/v = 0.7 \times 10^{-3}$.

For time windows larger than 10 days, the precision of the measurements rms(ϵ_{error}) is sufficiently smaller than the expected velocity drop. This indicates that using 21 well-distributed stations it is possible to study the velocity changes associated with the Wenchuan earthquake with a temporal resolution of less than 10 days, without further processing. However, it is clearly impossible to get a resolution of the order of 1 day, as in this case the expected uncertainties are larger than the velocity change.

To reach a temporal resolution that is sufficient to discriminate co-seismic from pre-seismic or post-seismic velocity changes, we need to improve the quality of the $\delta v/v$ measurements by increasing the coherency of the correlation functions. This is the subject of the next section.

5 IMPROVING THE MEASUREMENTS USING CURVELET DENOISING FILTERS

5.1 Basic assumptions

Our goal is to improve the temporal resolution of the velocity change measurements. For this, we attempt to increase the coherency between the reference correlation and the correlations computed with short time windows, which are referred to as the current correlation. In other words, we need to filter out all random fluctuations present in the current correlations that are not present in the reference correlation. This can be done by using the curvelet transform, as proposed by Stehly *et al.* (2011).

Let $\boldsymbol{C}(\tau_i, t_i)$ be a matrix that contains all of the current correlations computed between two stations. τ denotes the correlation time and t the calendar time. $\boldsymbol{R}(\tau_i, t_i)$ is a matrix of the same size as $\boldsymbol{C}$, each row of which is the reference correlation [see Figs 5(a) and

Downloaded from https://academic.oup.com/gji/article/201/3/1939/776465 by guest on 17 June 2021

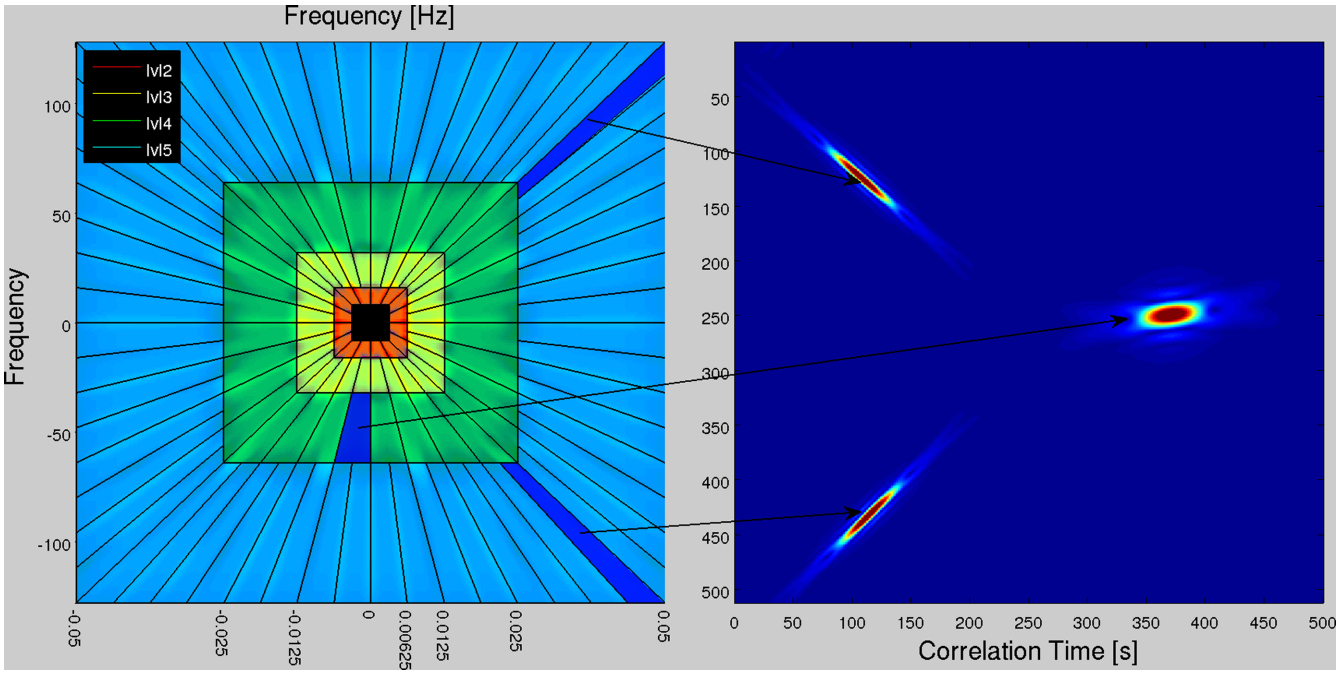

Figure 6. (a) Curvelets are constructed in the frequency domain by tiling the frequency plane with trapezoids: the inverse Fourier transform of each wedge is a curvelet in the physical space with a particular scale and orientation. Furthermore, the curvelet can be translated along the x and y axes. All of the curvelets of the same scale lie on the same ring in the frequency domain. We show in the frequency domain the curvelets of levels 2, 3, 4 and 5, in red, yellow, green and blue, respectiveley. (b) Curvelets frame elements are indexed by their level (scale) j, angle θ_l and position x, y. Here we show two curvelets in the physical space of level 5 (left) and one curvelet of level 4 (right). Each of these curvelets was obtained by taking the inverse Fourier transform of the wedge indicated with an arrow.

(b)]. Ideally, if all of the current correlations had converged towards the Green's function of the medium, $\boldsymbol{C}$ and $\boldsymbol{R}$ should be identical if there was no change in the medium.

In the following, we assume that $\boldsymbol{C}$ contains the same signal as $\boldsymbol{R}$ (which we consider as the best estimate of the Green's function), plus some random noise: $\boldsymbol{C} = \boldsymbol{R} + \boldsymbol{N}$, $\boldsymbol{N}$ being a zero-centred pseudo-noise. This is only valid if the following criteria are met:

(i) the velocity changes of the medium are small;
(ii) the distribution of noise sources only shows small short-term random fluctuations, and no strong systematic long-term variations.

5.2 The curvelet transform

To denoise $\boldsymbol{C}$, we take advantage of the properties of the curvelet transform, as proposed by Stehly *et al.* (2011).

Curvelets are designed to represent images in a transform space (Candès *et al.* 2006). Like the wavelet transform, it is a multiscale transform, but it uses a basis of functions that are simultaneously localized in frequency, physical space and orientation. Frame elements are indexed by their level or scale j, angle θ_l and position x, y. In physical space, they look like beams with different orientations and with limited extension. They are smooth in their direction of maximum extension, and they oscillate in the perpendicular direction [Fig. 6(b)].

Curvelets provide an optimally sparse representation of objects with edges and of wave propagators (Candes & Demanet 2004). For this reason, the curvelet transform is an ideal choice for detecting wave fronts and suppressing noise in seismic data (Herrmann *et al.* 2007), and as we shall see, in the noise correlation matrix.

As each row of the matrix $\boldsymbol{C}$ is a correlation, the x-axis of the physical space is the correlation time in seconds, and the y-axis is the calendar time. The correlations have a sampling rate of 5 Hz, and most of their energy is between 1–3 s periods.

5.3 Curvelet denoising filters

As shown in Fig. 5(b), all of the rows of $\boldsymbol{R}$ are identical, as they all contain the reference correlation that is a determinist signal that is expected to be close to the Green's function of the medium. The curvelet transform provides a sparse and compact representation of $\boldsymbol{R}$ that allows the definition of a mask in the curvelet domain from the amplitude of $\boldsymbol{R}$. This mask is then applied to $\boldsymbol{C}$ in the curvelet domain, and the filtered signals are transformed back into the time domain.

More precisely, we first compute the curvelet transform of the matrices $\boldsymbol{R}(\boldsymbol{\tau_i}, \boldsymbol{t_i})$ and $\boldsymbol{C}(\boldsymbol{\tau_i}, \boldsymbol{t_i})$. Let $\boldsymbol{r}_{j,l,x,y}$ and $\boldsymbol{c}_{j,l,x,y}$ be the coefficients of the curvelet transform of $\boldsymbol{R}$ and $\mathbf{C}$ at the scale j, angle θ_l and discrete position x, y. Separately, for each scale j and angle θ_l of the curvelet decomposition, we define a mask $\boldsymbol{r}^{\text{normalized}}_{j,l,x,y}$ by normalizing the coefficients $\boldsymbol{r}_{j,l,x,y}$ between 0 and 1.

The denoised correlation matrix is obtained by multiplying $\boldsymbol{c}_{j,l,x,y}$ by the mask $\left[\boldsymbol{r}^{\text{normalized}}_{j,l,x,y}\right]^n$. We then bring $\boldsymbol{C}$ back to the time domain. The user-defined parameter n modifies the strength of the filter. In our study, we choose $n = 0.5$.

Please note that since each row of $\boldsymbol{R}$ is identical, $\boldsymbol{r}_{j,l,x,y}$ has non-zero value only on the 'most vertical' curvelets. The efficiency of the denoising filter comes from two things:

Downloaded from https://academic.oup.com/gji/article/201/3/1939/776465 by guest on 17 June 2021

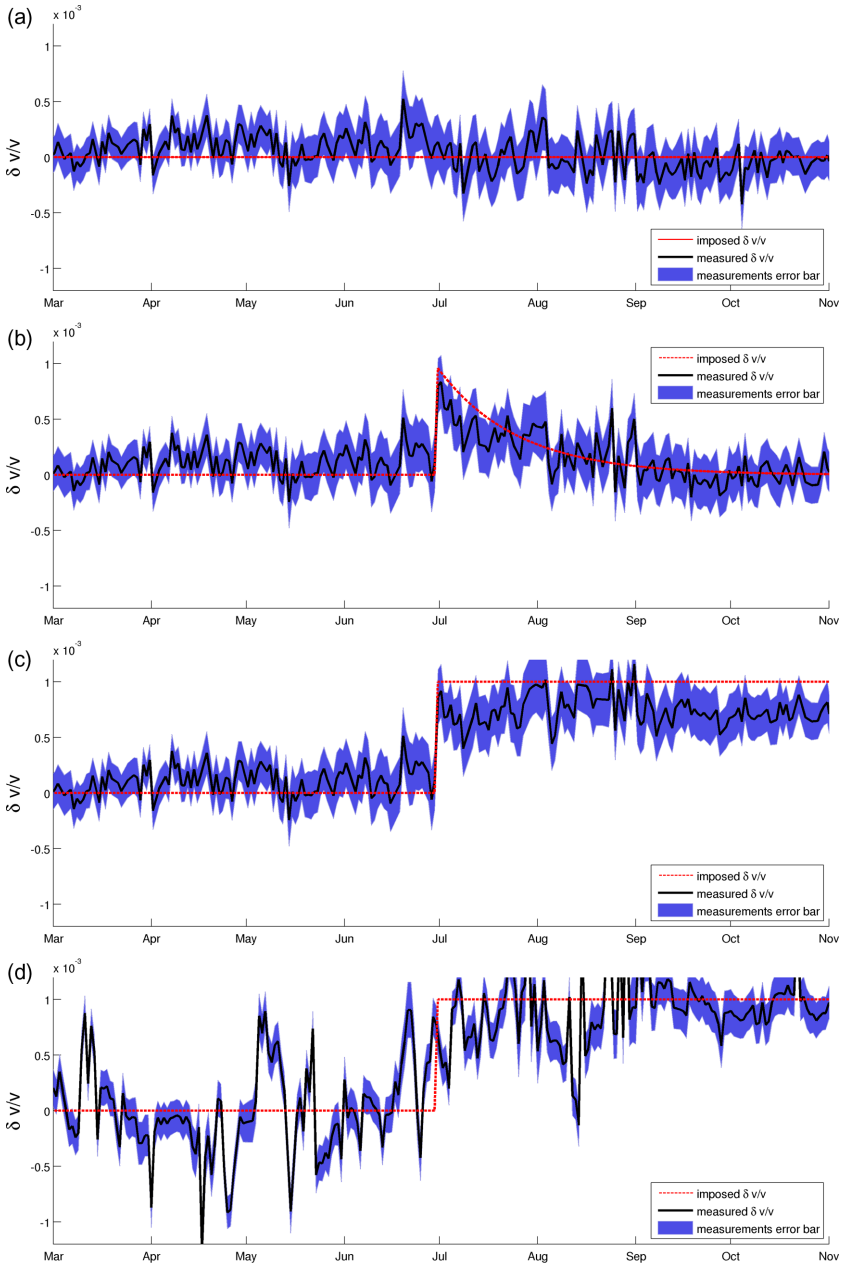

Figure 7. $\delta v/v$ measurement resolution tests using data recorded in 2007. Different scenarios are shown, where a seismic velocity variation in the medium is simulated by stretching the correlation coda waves (dashed red lines). The measured $\delta v/v$ is shown in black, and the blue shaded area corresponds to the error bar. (a) Simulation with no temporal variation and application of the curvelet denoising filter on the daily correlations. (b) As for (a), but with simulation of a temporal variation that consists of an abrupt velocity increase followed by exponential relaxation. (c) As for (b), but for a velocity change that consists of a step. (d) As for (c), but without using the curvelet denoising filter, and using a sliding window of 10 days.

(i) $\boldsymbol{C}$ is projected only on the 'most vertical' curvelets

(ii) The coefficients that are kept are filtered by the curvelet transform of the reference matrix.

The raw and 'denoised' matrix of the daily correlations for the station pair KCD01–KWC05 are shown in Figs 5(a) and (c), respectively. The denoised matrix looks smoother, although the most interesting point is that the sum of the raw and denoised correlations is exactly the same [Figs 5(a)–(c), lower panels]. This shows that the curvelet filter removed all of the signals that do not stack coherently from each of the daily correlations, while preserving the coherent signal.

5.4 Resolution test

The aim of this section is to evaluate the resolution of the $\delta v/v$ measurements carried out using the curvelet denoising filter. Moreover, we attempt to identify possible bias induced by this method. In particular, we would like to check if this denoising filter (1) 'smooths' the measured $\delta v/v$, which would give the illusion that the 'measured' seismic velocity variation starts before the 'real' seismic velocity variation; and (2) changes the magnitude of the observed $\delta v/v$.

To test the resolution of the $\delta v/v$ measurements, we use daily correlations computed using data recorded by the 21 stations in 2007. No major earthquakes occurred in 2007, so we assume that there is

Downloaded from https://academic.oup.com/gji/article/201/3/1939/776465 by guest on 17 June 2021

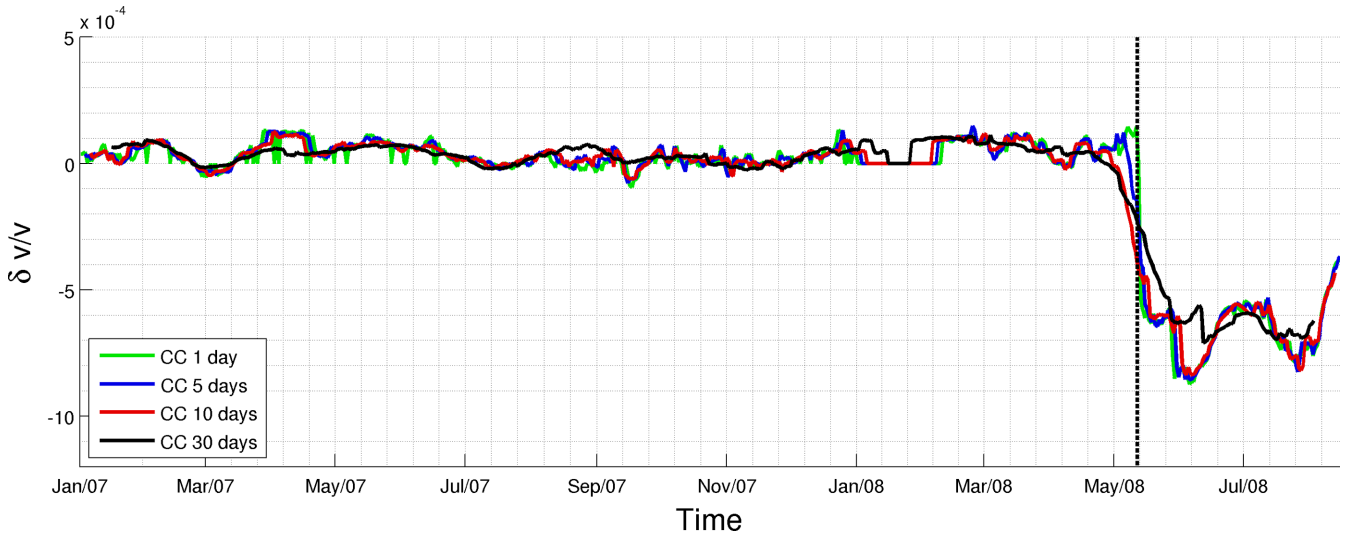

Figure 8. $\delta v/v$ measured by stretching on denoised correlations. Results obtained by using cross-correlations of 30, 10, 5 or 1 days of noise, shown in black, red, blue and green, respectively. The vertical dashed line indicates the day of the Wenchuan earthquake.

Table 2. Error on the measurements of the temporal evolution of the seismic wave velocity performed on the denoised correlations. Columns 2 and 3 indicate how the error on the dv/v measurements and the coherency between the reference correlation and the signal depend on the amount of noise correlated. Note that the velocity drop associated with the Wenchuan earthquake was about $\epsilon_0 = \delta v/v = 0.710^{-3}$.

Amount of noise correlated (days)	rms(ϵ_{error}) 10^{-3}	Average coherency
30	0.13	0.80
10	0.18	0.73
5	0.21	0.67
1	0.28	0.60

no significant seismic velocity change, although we cannot rule out the possibility that there were small velocity changes, associated for instance with hydrological loading (Meier *et al.* 2010; Froment *et al.* 2013), thermoelastic strain variations (Meier *et al.* 2010) or transient deformation (Rivet *et al.* 2014).

We simulate a seismic velocity variation $\delta v/v$ of 0.1 per cent by stretching the correlation codas. We then apply the curvelet denoising filter on daily correlations computed between each pair of stations and measure the $\delta v/v$. We test four scenarios:

(i) no change in velocity [Fig. 7(a)];
(ii) sharp increase in the velocity followed by exponential relaxation lasting 4 months [Fig. 7(b)];
(iii) a step-like velocity increase [Fig. 7(c)];
(iv) a step-like velocity increase as previously, but we do not apply the curvelet denosing filter, and we use correlations computed using a sliding window of 10 days [Fig. 7(d)].

Using the curvelet denoising filter, we can measure both a sudden increase in velocity as well as a long-term exponential decay. The measured velocity change starts exactly the same day as the imposed velocity change: the curvelet denoising filter does not smooth the result.

However, we can note that the curvelet filter induces a clear bias, as we tend to underestimate the magnitude of the velocity change. This is particularly visible when we impose a step function [Fig. 7(c)]; we measure a $\delta v/v$ of 0.07 per cent, whereas we imposed a $\delta v/v$ of 0.1 per cent.

5.5 Comparison of the curvelet transform with the S-transform

Baig *et al.* (2008) and Hadziioannou *et al.* (2011) used the S-transform (Stockwell *et al.* 1996) to increase the temporal resolution of seismic velocity change measurements. In their study of the 2004 September 24 Parkfield earthquake, and similar to our approach, Hadziioannou *et al.* (2011) used a correlation averaged over a long time window to denoise the daily correlations. They reported an increase in the temporal resolution from 30 days to 1 day.

The S-transform is a wavelet transform which brings a 1-D signal (for instance a correlation of 1 day) into a time–frequency space. In contrast, the curvelet transform brings a 2-D signal (a matrix of daily correlations) into a time/frequency/angle space. In our case, the frequency resolution is low, as our algorithm works essentially in a time/angle space. Both approaches are only effective if there are no strong seismic velocity or structural variations in the medium (so that the waveforms of the reference and the current correlation remain close to each other; see section 5.1), and no long-term and/or abrupt changes in the distribution of the noise sources (Hadziioannou *et al.* 2011).

6 RESULTS

We now apply the curvelet filter to the actual correlation functions. We consider correlations computed for all of the station pairs in the period that includes the Wenchuan earthquake. We measure the temporal velocity variation using the stretching method, as

Downloaded from https://academic.oup.com/gji/article/201/3/1939/776465 by guest on 17 June 2021

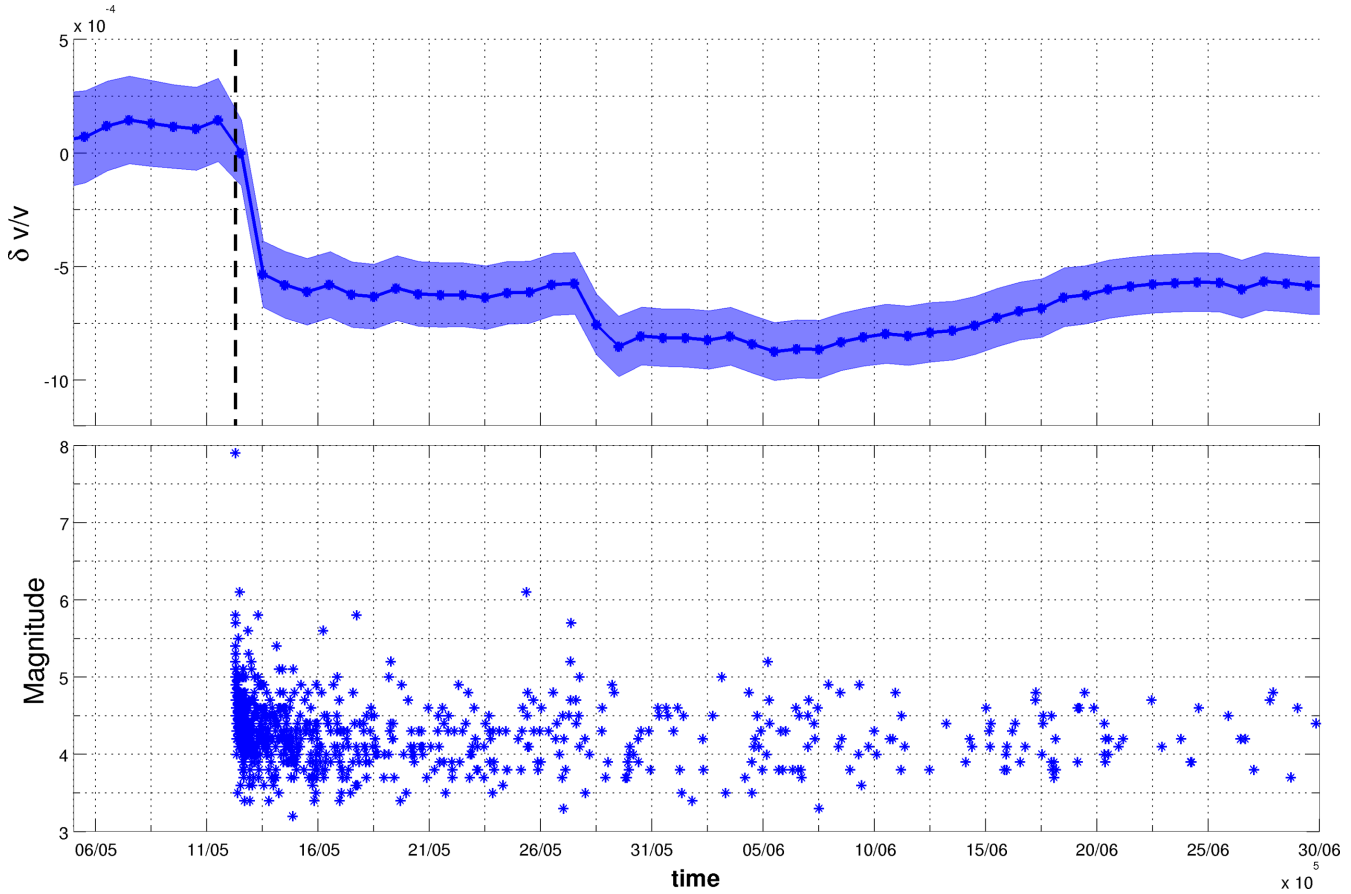

Figure 9. Upper panel: $\delta v/v$ measured using correlations of 1 day denoised using the curvelet transform (blue). The shaded area corresponds to the error bars computed using eq. (1). The vertical dashed line indicates the date of the Wenchuan earthquake. Due to the curvelet denoising filter, it is clear that the velocity drop starts the day of the Wenchuan earthquake, and lasts for about two days. There is a second smaller velocity drop on May 27–29. Lower panel: magnitude of the main shock and all of the aftershocks versus the time localized by the U.S. Geological Survey.

previously. The results are presented in Fig. 8 for correlations of 30, 10, 5 and 1 days.

The velocity drop associated with the Wenchuan earthquake can be clearly seen on all of the measurements. Its amplitude is similar to that which was observed with the 30-day correlations (see Fig. 4). Due to the curvelet denoising filter, we can now see how the velocity of the medium evolves over a short timescale, even with correlations of 1 day (Fig. 8, green). This was impossible with the raw correlations (Fig. 4). This illustrates that the curvelet filter successfully removes random fluctuations in the daily correlations, while keeping the useful coherent signal.

This is further illustrated in Table 2. The rms of the error in the estimation of dv/v using correlations of 30, 10, 5 and 1 days are 0.13×10^{-3}, 0.18×10^{-3}, 0.21×10^{-3} and 0.30×10^{-3}, respectively. On the one hand, the curvelet denoising filter does not improve the precision of the measurements performed using correlations of 30 days, but it does diminish the uncertainties by a factor of 4 on the measurements performed on the daily correlations.

Fig. 9 shows the dv/v measurements performed on the daily correlations with a zoom around the day of the Wenchuan earthquake. The shaded area corresponds to the error bars evaluated using eq. (1). It is now clear that the velocity drop started exactly on 2008 May 12, which is the day of the earthquake, and lasted until 2008 May 14. We can now see that 75 per cent of the velocity change occurred on 2008 May 12, so it is mostly co-seismic. This illustrates that the curvelet filter makes it possible to get more information from the data.

Moreover, there is a second smaller velocity drop of 0.025 per cent on 2008 May 27–29. This does not appear to be associated with aftershocks (Fig. 9, lower panel), as although there was a strong aftershock of magnitude 5.7 on 2008 May 27, this occurred more than 100 km away from the network of stations used.

6.1 Comparison of the seismic velocity variation measured in the 1–3 s and the 12–20 s period bands

Froment *et al.* (2013) showed that the Wenchuan earthquake was associated with a seismic velocity drop of 0.2 per cent in the 12–20 s period band, where the surface waves are mostly sensitive to the mid-crust at depths from 10 to 20 km.

Interestingly, they reported that this velocity change is delayed by at least 1 month relative to the time of the main shock. In contrast, in the 1–3 s period band, we found that the response of the medium to the earthquake was essentially co-seismic and had a smaller post-seismic component that was apparently delayed by only 1 day to 2 days.

This illustrates that the responses of the upper crust (which is sampled by the 1–3 s surface waves) and the mid-crust to the Wenchuan earthquakes were not characterized by the same timescale. Froment

Downloaded from https://academic.oup.com/gji/article/201/3/1939/776465 by guest on 17 June 2021

et al. (2013) suggested that in the 12–20 s period band the temporal variation of the seismic wave velocity is sensitive to visco-elastic relaxation of the deep crust and/or post-seismic slip. In the 1–3 s period band, different physical mechanisms can be invoked, such as poro-elastic relaxation in the brittle upper crust. The post-seismic velocity drop might also be associated with strong aftershocks.

CONCLUSION

Following Chen *et al.* (2010), we measured a velocity drop of 0.07 per cent associated with the Wenchuan earthquake, with a temporal resolution of about 10 days, using noise correlations computed between 21 stations that were ideally distributed around the Longmen Shan fault zone (Fig. 4).

To determine if this velocity drop occurred before, during, or after the main shock, we attempted to increase the temporal resolution of our observations. By taking advantage of the properties of the curvelet transform, we increased the signal-to-noise ratio of the daily correlations computed between each station pair. It was then possible to measure the velocity drop associated with the Wenchuan earthquake with a temporal resolution of 1 day. This shows that the velocity drop occurred on 2008 May 12, which is the day of the earthquake main shock (Fig. 9). Moreover, there was a second velocity drop of 0.025 per cent between 2008 May 27 and 29.

Although we successfully increased the temporal resolution of the dv/v measurements, it should be noted that our approach based on the curvelet transform is neither ultimate nor universal. It is not the ultimate method, in the sense that the curvelet transform was designed to provide sparse and compact representation of 2-D Green's functions. In our case, we used it with matrices where each line was a correlation; that is, a signal similar to a 1-D Green's function. This means that although we take advantage of the angular resolution of the curvelet transform, our way to use this is not optimal from a mathematical point of view.

Secondly, our approach is not universal, as it relies on strong assumptions: we assume that the velocity drop associated with the Wenchuan earthquake is small compared to the velocity of the medium, and that the noise sources do not have long-term variations. This last assumption implies that the curvelet denoising filter is likely to be useful only for periods shorter than 10 s, as longer period correlations show seasonal variations that clearly affect the noise correlations.

ACKNOWLEDGEMENTS

This study was partially supported by the ERC Advanced Grant WHISPER and the ANR 'HYDROSEIS' under the contract No. ANR-13-JS06-0004-01.

The authors thank Xavier Briand for his help with the data handling.

All of the seismic data used in this study come from stations belonging to the Western Sichuan Seismic Array (WSSA) that is operated by the Institute of Geology of the China Earthquake Administration.

REFERENCES

Baig, A., Campillo, M. & Brenguier, F., 2008. Enhancing seismic noise cross-correlations using data-adaptive filtering, *J. geophys. Res.,* doi:10.1029/2008JB006085.

Brenguier, F., Campillo, M., Hadziioannou, C., Shapiro, N., Nadeau, R. & Larose, E., 2008. Postseismic relaxation along the San Andreas Fault at Parkfield from continuous seismological observations, *Science,* **321**(5895), 1478–1481.

Candes, E. & Demanet, L., 2004. The curvelet representation of wave propagators is optimally sparse, *Commun. Pure appl. Math.,* **58,** 1472–1528.

Candès, E., Demanet, L., Donoho, D. & Ying, L., 2006. Fast discrete curvelet transforms, *Multiscale Modeling and Simulation,* **5,** 861–899.

Chen, J., Liu, Q.Y., Li, S.C., Guo, B., Wang, J. & Qi, S.H., 2009. Seismotectonic study by relocation of the Wenchuan M(s)8.0 earthquake sequence, *Chinese Journal of Geophysics-Chinese Edition,* **52,** 390–397.

Chen, J., Froment, B., Liu, Q. & Campillo, M., 2010. Distribution of seismic wave speed changes associated with the 12 May 2008 Mw 7.9 Wenchuan earthquake, *Geophys. Res. Lett.,* **37,** L18302, doi:10.1029/2010GL044582.

Corciulo, M., Roux, P., Campillo, M. & Dubucq, D., 2012. Instantaneous phase variation for seismic velocity monitoring from ambient noise at the exploration scale, *Geophysics,* **77**(4), Q37–Q44.

Froment, B., Campillo, M., Chen, J. & Liu, Q., 2013. Deformation at depth associated with the May 12, 2008 Mw 7.9 Wenchuan earthquake from seismic ambient noise monitoring, *Geophys. Res. Lett.,* **40,** 78–82.

Hadziioannou, C., 2011. Seismic waves in complex media: measuring temporal velocity variations, *PhD thesis,* University Joseph Fourier (Grenoble).

Hadziioannou, C., Larose, E., Coutant, O., Roux, P. & Campillo, M., 2009. Stability of monitoring weak changes in multiply scattering media with ambient noise correlation: laboratory experiments, *J. acoust. Soc. Am.,* **125,** 3688–3695.

Hadziioannou, C., Larose, E., Baig, A., Roux, P. & Campillo, M., 2011. Improving temporal resolution in ambient noise monitoring of seismic wave speed, *J. geophys. Res.,* **116**, doi:10.1029/2011JB008200.

Herrmann, F.J., Boeniger, U. & Verschuur, D., 2007. Nonlinear primary-multiple separation with directional curvelet frames, *Geophys. J. Int.,* **170,** 781–799.

Larose, E., Roux, P., Campillo, M. & Derode, A., 2008. Fluctuations of correlations and greens function reconstruction: role of scattering, *J. appl. Phys.,* **103**(11), 114907–114907-10.

Lobkis, O. & Weaver, R., 2003. Coda-wave interferometry in finite solids: recovery of p-to-s conversion rates in an elastodynamic billiard, *Phys. Rev. Lett.,* **90,** 254302, http://dx.doi.org/10.1103/PhysRevLett.90.254302.

Meier, U., Shapiro, N. & Brenguier, F., 2010. Detecting seasonal variations in seismic velocities within los angeles basin from correlations of ambient seismic noise, *Geophys. J. Int.*, **181**(2), 985–996.

Poupinet, G., Ellsworth, W. & Frechet, J., 1984. Monitoring velocity variations in the crust using earthquake doublets: an application to the Calaveras Fault, California, *J. geophys. Res.,* **89,** 5719–5731.

Rivet, D. *et al.*, 2014. Seismic velocity changes, strain rate and non-volcanic tremors during the 2009-2010 slow slip event in guerrero, mexico, *Geophys. J.,* **196**(1), 447–460.

Sabra, K., Roux, P. & Kuperman, W., 2005. Emergence rate of the time-domain Green's function from the ambient noise noise cross-correlation, *J. acoust. Soc. Am.,* **118**(6), 3524–3531.

Sens-Schönfelder, C. & Wegler, U., 2006. Passive image interferometry and seasonal variations at Merapi volcano, Indonesia, *Geophys. Res. Lett.,* **33,** L21302, doi:10.1029/2006GL027797.

Stehly, L., Campillo, M., Froment, B. & Weaver, R., 2008. Reconstructing green's function by correlation of the coda of the correlation (c3) of ambient seismic noise, *J. geophys. Res.,* **113,** B11306, doi:10.1029/2008JB005693.

Stehly, L., Cupillard, P. & Romanowicz, B., 2011. Towards improving ambient noise tomography using simultaneously curvelet denoising filters and SEM simulations of seismic ambient noise, *CRAS,* **343**(8), 591–599.

Downloaded from https://academic.oup.com/gji/article/201/3/1939/776465 by guest on 17 June 2021

Stockwell, R., Mansinha, L. & Lowe, R., 1996. Localization of the complex spectrum: the S transform., *IEEE Transactions on Signal Processing,* **44**(4), 998–1001.

Weaver, R.L., Hadziioannou, C., Larose, E. & Campillo, M., 2011. On the precision of noise correlation interferometry, *Geophys. J. Int.,* **185,** 1384–1392.

Wegler, U. & Sens-Schonfelder, C., 2007. Fault zone monitoring with passive image interferometry, *Geophys. J. Int.,* **168**(3), 1029–1033.

Xu, X., Wen, X., Yu, G., Chen, G., Klinger, Y., Hubbard, J. & Shaw, J., 2009. Coseismic reverse and oblique slip surface faulting generated by the 2008 Mw 7.9 Wenchuan earthquake, China, *Geology,* **37**(6), 515–518.

Zaccarelli, L., Shapiro, N.M., Faenza, L., Soldati, G. & Michelini, A., 2011. Variations of crustal elastic properties during the 2009 Laquila earthquake inferred from cross-correlations of ambient seismic noise, *Geophys. Res. Lett.,* **38,** L24304, doi:10.1029/2011GL049750.

Zhikun, L., Huang, J., Peng, Z. & Su, J., 2014. Seismic velocity changes in the epicentral region of the 2008 Wenchuan earthquake measured from three-component ambient noise correlation techniques, *Geophys. Res. Lett.,* **41,** 37–42.

Downloaded from https://academic.oup.com/gji/article/201/3/1939/776465 by guest on 17 June 2021